Origin of type-2 thermal-ion upflows in the auroral ionosphere

L. M. Kagan, J.-P. St.-Maurice

Annales Geophysicae (2005) 23: 13–24
SRef-ID: 1432-0576/ag/2005-23-13

Annales Geophysicae

Origin of type-2 thermal-ion upflows in the auroral ionosphere

L. M. Kagan[1,2] **and J.-P. St.-Maurice**[1]

[1]Department of Physics and Astronomy, University of Western Ontario, London, ON, Canada
[2]on extended leave from Radiophysical Research Institute (NIRFI), Nizhniy Novgorod, Russia

Received: 21 January 2004 – Revised: 28 June 2004 – Accepted: 15 July 2004 – Published: 31 January 2005

Part of Special Issue "Eleventh International EISCAT Workshop"

Abstract. The origin of thermal ion outflows exceeding 1 km/s in the high-latitude F-region has been a subject of considerable debate. For cases with strong convection electric fields, the "evaporation" of the ions due to frictional heating below 400–500 km has been shown to provide some satisfactory answers. By contrast, in the more frequent subclass of outflow events observed over auroral arcs, called type-2, there is no observational evidence for ion frictional heating. Instead, an electron temperature increase of up to 6000° K is observed over the outflow region. In this case, field-aligned electric fields have long been suspected to be involved, but this explanation did not seem to agree with expectations from the ion momentum balance. In the present work we provide a consistent scenario for the type-2 ion upflows based on our case study of an event that occurred on 20 February 1990. We introduce, for the first time, the electron energy balance in the analysis. We couple this equation with the ion momentum balance to study the salient features of the observations and conclude that type-2 ion outflows and the accompanying electron heating events are indeed consistent with the existence of a field-aligned electric field. However, for our explanation to work, we have to require that an allowance be made for electron scattering by high frequency turbulence. This turbulence could be generated at first by the very fast response of the electrons themselves to a newly imposed electric field that would be partly aligned with the geomagnetic field. The high frequencies of the waves would make it impossible for the ions to react to the waves. We have found the electron collision frequency associated with scattering from the waves to be rather modest, i.e. comparable to the ambient electron-ion collision frequency. The field-aligned electric field inferred from the observations is likewise of the same order of magnitude as the normal ambipolar field, at least for the case that we have studied in detail. We propose that the field-aligned electric field is maintained by the north-south motion of an east-west arc. The magnetic perturbation associated with the arc itself converts a small fraction of the perpendicular electric field into a field parallel to the total magnetic field, while the north-south motion ensures that the conversion never stops.

Key words. Ionosphere (Auroral ionosphere; Electric fields and currents; Ionosphere-magnetosphere interactions)

Correspondence to: L. M. Kagan
(lkagan@uwo.ca)

1 Introduction

Since their discovery 30 years ago (Shelley et al., 1972), numerous papers have been written on the presence of heavy ions (O^+ mostly) throughout the magnetosphere and on how they get there (e.g. Tsunoda et al., 1989; Hultqvist, 1991; Wahlund et al., 1992; and references therein). Since large fluxes of F-region ions have been seen moving upward along the geomagnetic field in the topside ionosphere, there is good reason to believe that such flows are at least initiated at relatively low ionospheric altitudes. It is also believed that actual ion injection into the magnetosphere requires a second ion acceleration mechanism operating at higher altitudes. Detailed studies of diurnal, seasonal, solar cycle and geomagnetic variations of ion outflows from F-region ionosphere may be found in Foster et al. (1998) and Liu et al. (2001).

Examples of relatively low altitude upward ion velocities ($V_{i\|}$) up to 2 km/s in magnitude have been reported by Whalen et al. (1978) from rocket observations at altitudes of 400 to 600 km. More recently, Wahlund and Opgenoorth (1989) and Wahlund et al. (1992) have also presented EISCAT incoherent-scatter radar measurements of thermal ion upflows (TIU) above the F-layer peak, with $V_{i\|}$ values increasing rapidly with altitude and achieving speeds of the order of 1 km/s.

Wahlund et al. (1992) have classified the TIU events into two types. The type-1 TIU event is associated with a strong convection electric field, elevated ion temperature T_i, a "lifted F-layer", and almost no auroral precipitation. This type seems to account for an enhanced pressure gradient directed along the geomagnetic field **B**. The gradient is produced by ion frictional heating and results in an upward motion of the expanding thermal plasma (Loranc et al., 1991; Loranc and St-Maurice, 1994; Wilson, 1994).

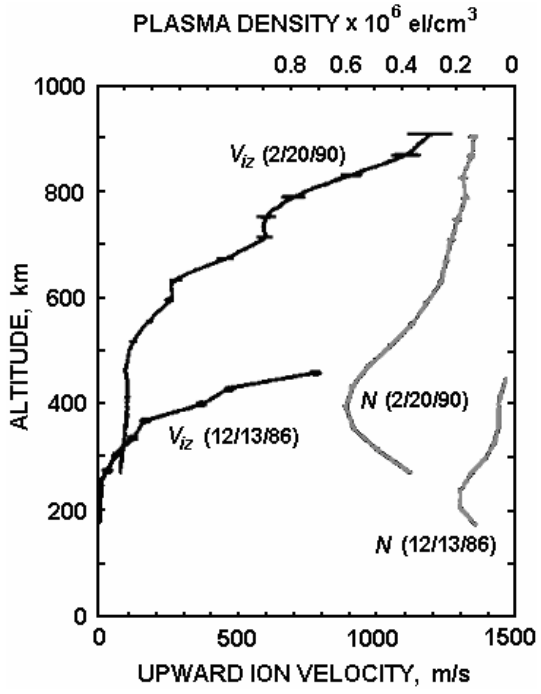

Fig. 1. Profiles of the field-aligned ion drift, $V_{i\|}$, and of the electron density, N, for two type-2 TIU events, one from 17:57 UT on 13 December 1986, during a period of low solar activity and the other from 22:13 UT on 20 February 1990, for a period of high solar activity. From (Wahlund and Opgenoorth, 1989) and (Wahlund et al., 1992).

The type-2 TIU event is associated with energetic electron precipitation, auroral arcs, a weak convection electric field, an elevated electron temperature T_e but no elevated T_i, and with either a decreased or a normal looking plasma density N in the topside F-layer. Of the two types, the second is usually stronger and occurs more frequently than the first.

Wahlund et al. (1992) suggested that type-2 events were perhaps a result of an enhanced field-aligned electric field $E_\|$ and speculated that such a field could be produced by anomalous resistivity associated with low-frequency plasma turbulence. However, this conclusion was not consistent with the pressure gradients being observed, and there was no discussion as to the origin of the mysterious field-aligned electric field or its value, for that matter. The source of turbulence, furthermore, was not identified. The upshot is that the mechanism that drives type-2 TIU events, a major supplier of heavy ions to the magnetosphere, isn't yet identified clearly and/or convincingly.

Additional clues as to the origin of type-2 TIU events might be found in what seems to be very much a related phenomenon (perhaps differing in the strength of the driving mechanism), namely, enhanced ion-acoustic fluctuations in the F-region. Forme et al. (1995) and Forme and Fontaine (1999) have studied the occurrence of these fluctuations and identified two types. Their first type, in particular, was associated with large upward ion velocities, strongly enhanced electron temperatures, auroral arcs with precipitating particles in the 100 eV to 10 keV energy range, and with an altitude extent covering the upper F-region between 300 and 700 km. The arcs were also observed to move southward with a velocity of about 100 m/s. This is very much in line with the morphology of type-2 ion outflow, as classified by Walhlund et al. (1992). Indeed, Forme and Fontaine (1999) analyzed the electron temperature profiles when such temperatures had pronounced local maxima during enhanced ion acoustic echo events and came to the conclusion that there were two parameters which were enhanced well above the normal level, namely, the electron temperature and the ion field-aligned velocity. Both are signatures of type-2 TIU events.

Note that since the standard procedure couldn't be used for regions of enhanced ion acoustic echoes, Forme and Fontaine (1999) developed a special algorithm to estimate the electron temperature located within the regions of ion acoustic turbulence by identifying the position of each ion-acoustic peak during unstable situations. Their method showed that in the turbulent regions the electron temperature may reach up to 11 000° K while the ion outflow velocities were able to reach 1300 m/s at 800 km. The ions seemed to be accelerated by the field-aligned electric field that was due to the electron temperature gradient.

In this paper we go back to less extreme type-2 TIU events which have neither been accompanied by prominent ion-acoustic turbulence nor have exhibited clear maxima in the electron temperature altitude profiles. We give a quick overview of type-2 TIU events in Sect. 2. We present a quantitative analysis of one TIU event processed on 20 February 1990 in Sect. 3. We end with our discussion and conclusion in Sect. 4.

2 An overview of type-2 TIU events

In Fig. 1 we produce examples of ion outflows, $V_{i\|}$, and of the electron density data from published TIU events observed with the EISCAT radar. The two events shown were obtained at 17:57 UT on 13 December 1986, during a period of low solar activity (Wahlund and Opgenoorth, 1989) and at 22:13 UT on 20 February 1990, for a period of high solar activity (Wahlund et al., 1992). The profiles illustrate the significant increase in the magnitude of $V_{i\|}$ with altitude. In both cases the magnitude of $V_{i\|}$ increases dramatically a few hundred km above the F-peak, in spite of very different density peak values and positions.

A feature that distinguishes type-2 from type-1 TIU events is their close association with enhancements in T_e but not in T_i. This relationship can be seen in Fig. 2, where we have reproduced the observed values of T_e and T_i for the events shown in Fig. 1 and for another event as well. On 20 February 1990, in particular, T_e reached 6000° K at 900 km altitude while T_i varied between 1000 and 2000° K, which is typical for periods of high solar activity in a quiet ionosphere. Likewise, on 13 December 1986, T_e reached 4000° K while T_i

remained below 1000° K (Wahlund and Opgenoorth, 1989). The latter is typical of quiet periods with low solar activity. In both instances, the low values of T_i, particularly below 400 km, indicate that there was little ion frictional heating and that the regions were therefore devoid of large perpendicular convection electric fields during the type-2 TIU events.

The most plausible explanations for the enhanced T_e values during the TIU events would have to be one of the following: heating in association with soft electron precipitation, heat conduction from above, or heating by friction with ions in the presence of acceleration by a field-aligned electric field or some other force responsible for the creation of intense field-aligned current densities. Of these three possibilities, soft electron precipitation has to be ruled out because the temperature keeps increasing with height well above the F-peak and well above the region where soft electrons normally deposit their energy. Likewise, we show below that conduction from above also has to be ruled out because the vertical temperature gradients seem to be too weak to account for a transfer of heat that would be fast enough to provide the observed temperatures. This leaves localized field-aligned electric fields (and attendant regions of intense field-aligned current densities) as the next most plausible alternative. We show below that the observations on 20 February 1990 appear to be consistent with this notion.

While ground-based observations are able to provide a quantitative determination of ion and electron temperatures and ion upflows, the determination of intense field-aligned current densities is more indirect and, therefore, debatable. However, the correspondence between magnetic perturbations and simultaneous ion outflows is obtained less ambiguously and far more precisely with in-situ satellite or rocket observations. We provide an example of a satellite observation of the connection between $V_{i\parallel}$ and the localized upward field-aligned current (FAC) regions in Fig. 3, where we have reproduced the downward component of the ion velocity ($V_{\rm down}$) and the simultaneous eastward magnetic perturbation, B_x, measured by the Hilat satellite on 1 March 1984. This was one of two specific examples presented in Tsunoda et al. (1989). For the purpose at hand we can interpret the increase in universal time (UT) as an increase in geomagnetic latitude (from left to right). The region of enhanced $V_{\rm down}$ is then seen to be bounded in latitude. The time interval from 16:19:30 to 16:20:00 UT corresponds to a latitudinal width of about 2°. Negative values of $V_{\rm down}$ are essentially equal to upward $V_{i\parallel}$ values. The triangular shaped magnetic perturbation curve is usually interpreted simply in terms of two infinite FAC ($j_\parallel$) sheets, with $j_\parallel$ directed downward in the positively sloped region and upward in the negatively sloped region (e.g. Iijima and Potemra, 1976). These signs are indicated by the arrows in Fig. 3 (the zonal magnetic perturbation B_x is eastward when the upward FAC is poleward of the downward FAC, but is westward when their relative locations are reversed).

The obvious point about Fig. 3 is that the upward $V_{i\parallel}$ region, accentuated by the shaded band, is spatially coincident with the upward current region. A similar strong trend for a connection between large ion outflows and intense upward field-aligned currents was noted by Tsunoda et al. (1989) on a study of several Hilat passes on the dayside near 800 km. Interestingly enough, strong $|V_{i\parallel}|$ values, in excess of 1 km/s, and their occurrence in a region of intense field-aligned currents, are highly reminiscent of radar TIU observations while both sets of observations do suggest a connection with field-aligned electric fields at ionospheric heights.

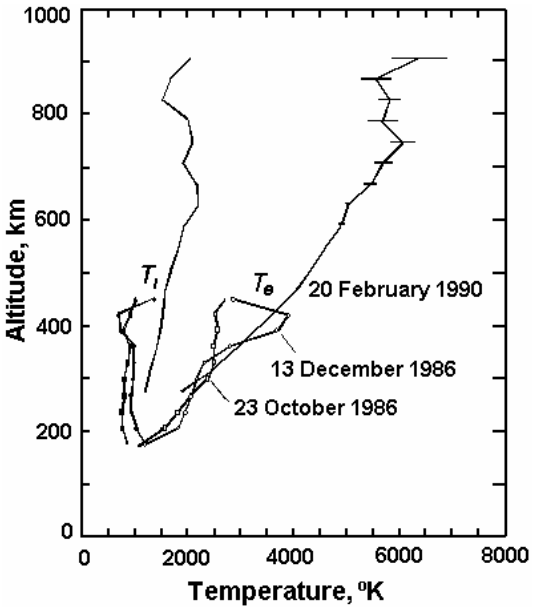

Fig. 2. Profiles of the electron temperature, T_e, and the ion temperature, T_i, associated with the $V_{i\parallel}$ and N profiles in Fig. 1. Also, temperature profiles for 23 October 1986. From Wahlund and Opgenoorth (1989) and Wahlund et al. (1992).

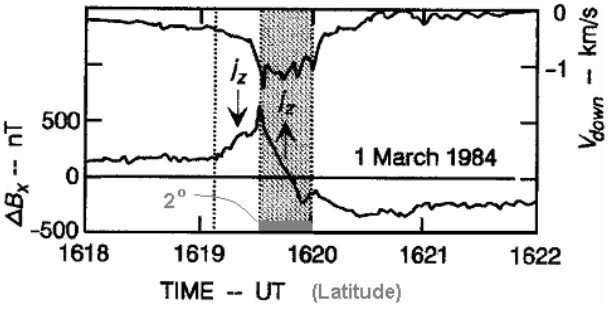

Fig. 3. Downward component of the ion velocity ($V_{\rm down}$) and simultaneous eastward magnetic perturbation, B_x, measured by the Hilat satellite on 1 March 1984. From (Tsunoda et al., 1989).

3 Detailed case study analysis of one TIU event

In order to further our understanding of TIU events we have made a detailed quantitative study of the spectacular type-2 TIU event observed on 20 February 1990 at 22:13 UT. We already introduced this event in Figs. 1 and 2. The observations

of the topside ionosphere were carried out with the UHF (933 MHz) and VHF (224 MHz) EISCAT radars pointing, respectively, along the magnetic field and vertically. More details on the experiment may be found in Wahlund et al. (1992).

We start our study with the simplest possible mathematical model that could be used to describe such a system, namely, a steady-state quasi-neutral two-fluid plasma description based on the ion and electron momentum balance and the electron energy balance (type-2 TIUs are devoid of ion heating signatures and do not require the inclusion of the ion energy balance).

We consider electron and ion momentum equations:

$$-e\nabla p_e - Ne^2\mathbf{E} + Nm\mathbf{g}e \cong m\omega_e\mathbf{j_e}\times\mathbf{b} - e\mathbf{R_u} + e\mathbf{R_T} \quad (1)$$

$$-e\nabla p_i + Ne^2\mathbf{E} + NM\mathbf{g}e \cong -M\omega_i\mathbf{j}_i\times\mathbf{b} + e\mathbf{R_u} + Mv_{in}^*\mathbf{j}_i - e\mathbf{R_T}, \quad (2)$$

where

$$v_{in}^* = v_{in} + V_i\cdot\nabla; \quad (3)$$

To this we add the constraint of divergence free currents:

$$\nabla\cdot N\mathbf{V_e} = \nabla\cdot N\mathbf{V}_i, \quad (4)$$

the electron energy balance equation:

$$\frac{3}{2}Nk_T\left(\frac{\partial T_e}{\partial t} + \mathbf{V}_e\cdot\nabla T_e\right) + Nk_T T_e\nabla\cdot\mathbf{V}_e + \nabla\cdot\mathbf{q_e}$$

$$= -\frac{3m}{M}N\nu_{ei}k_T(T_e - T_i) + (\mathbf{R_u} + \mathbf{R_T})\cdot\mathbf{u} \quad (5)$$

and Ampere's law:

$$\nabla\times\mathbf{B} = \mu_0\mathbf{j}. \quad (6)$$

Here e denotes the magnitude of the electron charge; p_e and p_i, N, and $\mathbf{E}$ are the electron and ion pressure, the plasma density and the vector electric field, respectively; $\mathbf{g}$ is the gravitational acceleration; m and M are electron and ion masses; e is the magnitude of the electron charge; $\mathbf{j}_e$=e$\mathrm{N}\mathbf{V}_e$ and $\mathbf{j}_i$=e$\mathrm{N}\mathbf{V}_i$ are the electron and ion current densities, so that $\mathbf{j}$= $\mathbf{j}_i-\mathbf{j}_e$; ν_{ei} and ν_{in} are electron-ion and ion-neutral collisional frequencies; ω_e and ω_i are the electron and ion gyrofrequencies; $\mathbf{b}$=$\mathbf{B}/B_0$ is a unit vector along the total magnetic field; μ_0 is the permittivity of free space; $\mathbf{R}_u$ is the frictional force; $\mathbf{R}_T$ is the thermal force; $\mathbf{u}$=$\mathbf{V}_i-\mathbf{V}_e$ is the current velocity, i.e. the relative velocity between ions and electrons, so that $\mathbf{j}$=e$\mathrm{N}\mathbf{u}$; $\mathbf{q}_e$ is the electron heat flux and and k_T is the Boltzman constant. Note that we have neglected electron-neutral collisions in Eqs. (1) and (3) since $\nu_{ei}\gg\nu_{en}$ at the altitudes of interest.

In the following we find the altitude behavior of the field-aligned current density and of the field-aligned electric field based on the observations of the type-2 TIU event on 20 February 1990. For this purpose, we have calculated collision and gyro-frequencies using the MSIS-E and IGRF models from the NASA/Goddard Flight Center web site http://nssdc.gsfc.nasa.gov/space/model/. We also have produced a quadratic interpolation of the $V_{i\|}$ and T_i altitude profiles, and have interpolated the plasma density N data using a Chapman layer type of description. This fitting has been done to make it possible to obtain the necessary derivatives free of artificial noise. The electron temperature T_e profile could be fitted equally well with a second order polynomial and a logarithmic interpolation. We chose the logarithmic fit to avoid a sudden and probably artificial change in the sign of the first and second T_e derivatives. Put in another way: we saw no reason to assume that T_e reached a maximum near the highest altitudes available. This being stated, since these two T_e interpolations did fit the data equally well, we have presented the consequences of the T_e quadratic interpolation in Appendix A.

3.1 Questions raised by the standard ion momentum balance

In the two-fluid model for thermal electrons and ions, the field-aligned ion velocity can be found by summing Eqs. (1) and (2) and taking the component of the ion velocity along the total geomagnetic field:

$$V_i\cdot b = V_{i\|} = -\frac{\nabla_\|(p_e + p_i)}{MN\nu_{in}^*} + \frac{g\cos D}{\nu_{in}^*}. \quad (7)$$

Here ν_{in}^* includes both ion-neutral collisions through the collision frequency ν_{in} and ion inertia while the subscript $\|$ denotes the geomagnetic field direction.

The advantage of using Eq. (7) is that the variations in the ion density and the ion and electron temperatures are provided by the incoherent radar data. We can therefore check if the balance predicted by Eq. (7) is consistent with the observations of density and temperatures along the geomagnetic field lines. The result of that part of our study is shown in Fig. 4 under the assumption that the observed pressure variations indicate changes that are occurring strictly along the magnetic field. That is not strictly true, since the radar beam is rigorously parallel to the geomagnetic field lines only near 250 km altitude. Near the higher altitudes of the observations, the radar actually targets other magnetic field lines approximately 150 km away by the time we reach 900 km altitude.

From Fig. 4 it can be seen that, for the event at hand, at least, there was a reasonably good balance up to 750 km altitude between the gravitational acceleration term (bottom line with hollow triangles) and the pressure gradient-driven term that contained both the ion and electron pressures (top line with hollow squares). This is reflected by the fact that the sum of these two terms (solid line) should have to produce flows of the order of $\pm$100 m/s. According to that balance, furthermore, the ions should have been moving downward above 750 km altitude. This is in stark contrast with the observation of a steady increase in the upward ion drift, which reached as much as 1200 m/s (black dots) at the upper altitudes.

We can only conclude at this juncture that there is something fundamentally wrong with the simple, yet very standard, model of ion and electron momentum balance. This is not an artifact of our interpolation procedure or of our model parameters. Wahlund et al. (1992) also found that the pressure gradient could not account for the thermal ion outflows and concluded from this that the mechanism responsible for TIU-2 remained basically unknown, in spite of the fact that they strongly suspected that field-aligned electric fields were involved.

The trouble with our momentum equations as they currently stand is that the ions feel the presence of any field-aligned electric field through the electron pressure gradient term: when we take a sum of the electron and ion momentum balances, the effects of currents cancel one another (there can be no acceleration of the center of mass through mutual collisions) while the effect of gravity on electrons is negligible when compared to ions. Since the observations are telling us that the electron pressure gradient is not large enough to account for the ion motion, we then have only two possibilities left. Either there is a third species in the system, aside from thermal electrons and ions, or there is a form of scattering that does not involve a direct interaction between ions and electrons. In the first instance we can think of precipitating and "runaway" (that is, superthermal) electrons being accelerated by a field-aligned electric field without colliding with the ions, owing to the small collision cross sections associated with their large speeds. In the second case we have to postulate some high-frequency turbulence that would be able to scatter the very electrons that are trying to short out the field-aligned electric field but that doesn't affect the ions. The high frequencies mean that the turbulence has no impact on the ions (with their large inertia, the ions are unable to react to high frequency fields). As a result, the ions would be capable of responding directly to the field-aligned electric field because the electrons would be impeded by the turbulent wave fields. To study our two hypotheses in more detail, we need more information. Otherwise, we have, for example, too many combinations of field-aligned electric fields and effective electron collision frequencies to choose from. This is where a study of the electron energy balance comes in handy. The electron temperature is telling us about the electron frictional rate, which in turn tells us something about the relative electron-ion drift and, therefore, the field-aligned electric fields. Therefore, before continuing with our investigation of the ion momentum balance we turn first to the electron energy balance, in order to see what constraints it introduces on the acceleration mechanisms that we wish to study. Once this is done, and once we have uncovered the magnitude of the field-aligned fields involved, we can try to figure out the origin of these field-aligned electric fields, a task that we carry out in the final part of this paper.

3.2 What is learned from the electron thermal balance

Upper F-region electrons are collisional. In the absence of plasma turbulence Ohmic heating comes from frictional heating between electrons and ions, which can create elevated electron temperatures. The electron heating process in the ionospheric F-region is described in this case by the electron thermal conductivity Eq. (3) in which the various forcing and heat flow terms are (e.g. Huba, 2000)

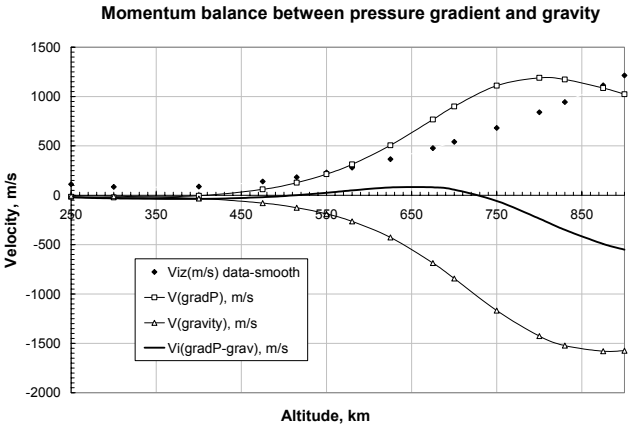

Fig. 4. Contributions to the field-aligned ion velocity found in a steady-state quasi-neutral two-fluid plasma description. A reasonable balance is seen up to 750 km altitude between the gravitational acceleration term (bottom line with hollow triangles) and the electron plus ion pressure gradient term (top line with hollow squares). A balance between gravity and the pressure gradient term (solid line), should have to produce flows of the order of ± 100 m/s with a downward ion motion above 750 km altitude. This is in stark contrast with the observation of a steady increase in the upward ion drift (black dots).

$$\mathbf{R_u} \cong N m \nu_{ei} (0.51 \mathbf{u}_{\parallel} + \mathbf{u}_{\perp}), \tag{8}$$

$$\mathbf{R_T} \cong -0.71 N k_T \nabla_{\parallel} T_e - \frac{3}{2} N \frac{\nu_{ei}}{\omega_e} k_T (\mathbf{b} \times \nabla_{\perp} T_e), \tag{9}$$

$$\mathbf{q_e} \cong \mathbf{q}_u^e + \mathbf{q}_T^e, \tag{10}$$

where

$$\mathbf{q}_u^e = 0.71 N k_T T_e \mathbf{u}_{\parallel} + \frac{3\nu_{ei}}{2\omega_e} N k_T T_e (\mathbf{b} \times \mathbf{u}_{\perp}) \tag{11}$$

is the frictional heat flux and

$$\mathbf{q_T^e} = -3.2 \frac{N k_T T_e}{m \nu_{ei}} k_T \nabla_{||} T_e - 4.7 \frac{N k_T T_e \nu_{ei}}{m \omega_e^2} k_T \nabla_{\perp} T_e$$

$$- 2.5 \frac{N k_T T_e}{m \omega_e} k_T (\mathbf{b} \times \nabla_{\perp} T_e) \tag{12}$$

is the thermal gradient heat flux. Here the subscripts $\parallel$ and $\perp$ denote the components along and perpendicular to the total magnetic field **B**. With Eq. (8) we can easily recognize the first and the second terms on the RHS of Eq. (3) as being the collisionally-driven electron cooling and heating rates, respectively.

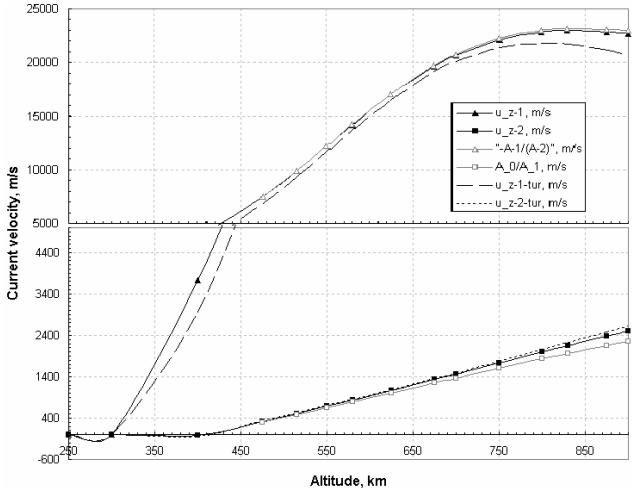

Fig. 5. The two $u_\parallel$ solutions (lines with full triangles and squares) found from the electron energy balance (Eq. (15)) as functions of altitude at 22:13 UT on 20 February 1990. Calculations made using altitude profiles for N, T_e, T_i and $V_{i\parallel}$ interpolated from Fig. 9 in Wahlund et al. (1992). The approximate solutions to Eq. (15) (lines with hollow triangles and squares) show a very good fit to the exact ones. The two solutions for the current velocity in the presence of high-frequency turbulence (broken and dashed lines) are very similar to those obtained without the turbulent contributions (lines with full triangles and squares).

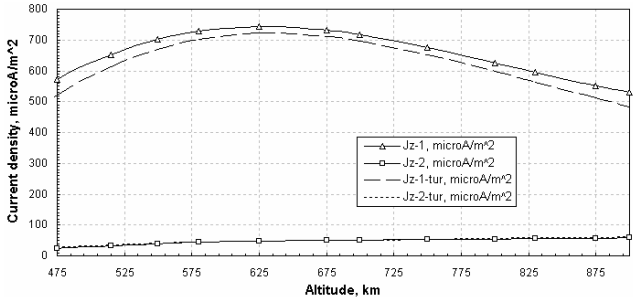

Fig. 6. Current densities corresponding to the two $u_\parallel$ solutions shown in Fig. 5, without (lines with hollow triangles and squares) and with (broken and dashed lines) high-frequency turbulence.

With the above expressions, using Eq. (4), neglecting perpendicular gradient terms and substituting $V_{e\parallel}=V_{i\parallel}-u_\parallel$ we can rewrite Eq. (3) as

$$\begin{array}{l} 0.51Nmv_{ei}u_\parallel^2+(1.5Nk_T\nabla_\parallel T_e-T_ek_T\nabla_\parallel N)u_\parallel \\ -(1.5Nk_T\nabla_\parallel T_e-T_ek_T\nabla_\parallel N) \\ V_{i\parallel}-\frac{3m}{M}Nv_{ei}k_T(T_e-T_i) \\ +3.2\frac{k_T^2}{m}\nabla_\parallel\left(\frac{NT_e}{v_{ei}}\nabla_\parallel T_e\right)=0. \end{array} \tag{13}$$

The electron-ion collision frequency in Eq. (13) is a function of ion density and electron temperature, and may be written as (Shunk and Nagy, 2000)

$$v_{ei}\cong 54.5\,N\,T_e^{-3/2}, \tag{14}$$

as long as v_{ei} is expressed in s^{-1}, N is in cm^{-3} and T_e is in $^\circ$K.

Equation (13) is a quadratic equation that can be solved for $u_\parallel$ since all other parameters are either measured or may be calculated from models and/or from the data. In other words, in the absence of turbulent effects, the altitude dependence of $u_\parallel$ is given by

$$u_\parallel^{1,2}=\frac{1}{2A_2}\left\{-A_1\pm\sqrt{A_1^2-4A_0A_2}\right\}, \tag{15}$$

where

$$A_2=0.51Nmv_{ei} \tag{16}$$

$$A_1=1.5Nk_T\frac{\partial T_e}{\partial z'}-k_TT_e\frac{\partial N}{\partial z'} \tag{17}$$

$$\begin{array}{l} A_0=-A_1V_{iz'}-\frac{3m}{M}Nv_{ei}k_T(T_e-T_i) \\ +0.059\frac{k_T^2}{m}\left[2.5\,T_e^{3/2}\left(\frac{\partial T_e}{\partial z'}\right)^2+T_e^{5/2}\frac{\partial^2T_e}{\partial z'^2}\right]. \end{array} \tag{18}$$

Here we used the symbol z' to describe the gradients along the total magnetic field $\mathbf{B}$ (z is the direction along the unperturbed geomagnetic field $\mathbf{B_0}$).

In Fig. 5 we plot the two $u_\parallel$ solutions given by Eq. (15) as functions of altitude for 22:13 UT. The solutions were calculated using the interpolated altitude profiles of N, T_e, T_i and $V_{i\parallel}$ from Fig. 9 in Wahlund et al. (1992) and using v_{ei} from Eq. (14). However, one of the solutions, $u_{\parallel,1}$, (black curve with full triangles) gives an unrealistically high current density $j_\parallel=eNu_\parallel$, namely, gives a field-aligned current varying between 354 and 743 μA/m^2 (Fig. 6). Given that we are not dealing with a particularly narrow region or currents here, we have excluded this solution from further consideration. The other solution, $u_{\parallel,2}$, is associated with a current density varying between 24 and 58 μA/m^2. From Fig. 5 it is seen that electron frictional heating (the term proportional to u^2) is not important for this solution.

The great advantage of having used the electron energy balance is that, knowing $u_\parallel$ and neglecting the effect of gravity on electrons, we may also derive the field-aligned electric field from Eq. (1):

$$E_\parallel\cong-\frac{\nabla_\parallel p_e}{Ne}-0.71\frac{k_T\nabla_\parallel T_e}{e}+\frac{mv_{ei}}{e}u_\parallel. \tag{19}$$

This field-aligned electric field is shown in Fig. 7. The line with hollow squares corresponds to the $u_{\parallel,2}$ solution; the line with hollow triangles is for the $u_{\parallel,1}$ solution.

With this information on the field-aligned electric field, we can now return to the ion momentum balance and study the possibility that runaway or even precipitating electrons could be responsible for the large field-aligned ion drifts that were observed.

3.3 The third species possibility

Since the radar measurements come from the ion line, we pretty much have to assume that any missing species from our equations has to be made of non-thermal electrons. Such electrons have no influence on the spectral shape, unless they trigger low frequency plasma instabilities (not seen in this instance anyway). These non-thermal electrons could either be precipitating electrons or "runaways".

Using the symbols N^{nt} for the non-thermal electrons and N^{th} for the density of the thermal electrons the three-fluid set of momentum equations along the geomagnetic field becomes

$$-N^{nt}eE_{\parallel} \cong mN^{nt}(\mathbf{V}_e^{nt}\cdot\nabla)V_{e\parallel}^{nt}, \tag{20}$$

$$-\nabla_{\parallel}p_e^{th} - N^{th}eE_{\parallel} \cong -0.51mv_{ei}N^{th}u_{\parallel} - 0.71N^{th}k_T\nabla_{\parallel}T_e, \tag{21}$$

$$-\nabla p_i + NeE_{\parallel} + NMg\cos D \cong 0.51mv_{ei}N^{th}u_{\parallel} + Mv_{in}^{*}NV_{i\parallel} + 0.71N^{th}k_T\nabla_{\parallel}T_e, \tag{22}$$

where $N{=}N^{nt}{+}N^{th}$ is the ion density. In Eq. (20) the pressure gradient term has been replaced, for the non-thermal electrons, by the nonlinear acceleration term, while friction has been dropped owing to the very small collision frequency of fast electrons. In effect, we are assuming by writing Eq. (20) that the non-thermal population involved would behave the same way as individual particles falling through a field-aligned potential drop.

There are two problems that immediately make the non-thermal electrons a very doubtful possibility. The first has to do with the potential drop associated with the electric fields derived in Fig. 7. Even for the larger of the two possible values the total drop is less than 2 V. With the more likely small parallel electric field possibility it is actually less than 0.5 V. These values are too small to consider that electrons undergoing such a change in potential should be considered as truly suprathermal.

The second problem is related to the first but provides a different view point, namely, we obtain a suprathermal population that is too large to make sense. To reach this result, we start by adding Eqs. (20)−(22) so as to obtain an expression for the field-aligned ion velocity. Since the sum of the pressure gradients from thermal electrons and ions is roughly balanced by gravity (Sect. 3.1) we arrive at

$$V_{i||} \cong -\frac{N^{nt}\nabla_{||}(mV_{e||}^{nt}2/2)}{MNv_{in}^{*}}. \tag{23}$$

Using Eq. (20) we can replace the numerator of Eq. (23) by the field-aligned electric field to obtain

$$V_{i||} \cong \frac{eE_{||}}{Mv_{in}^{*}}\frac{N^{nt}}{N}. \tag{24}$$

Since the electric field has been obtained from the thermal electron energy balance, and with the observations of the field-aligned ion drift, we can obtain from this the density of non-thermal electrons, namely,

$$N^{nt} = N\frac{V_{i||}Mv_{in}^{*}}{eE_{||}}. \tag{25}$$

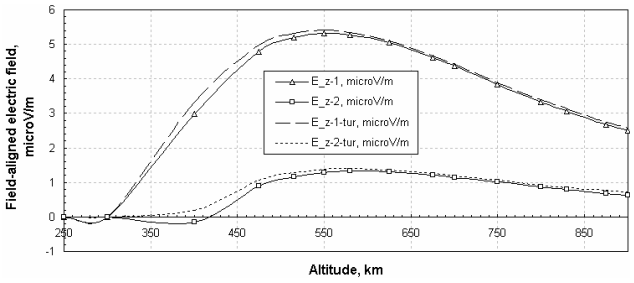

Fig. 7. Field-aligned electric field corresponding to the two $u_{\parallel}$ solutions from Fig. 5 without (lines with hollow triangles and squares) and with (broken and dotted lines) high-frequency turbulence.

For the smaller electric field derived from the electron energy balance (our second current velocity solution with its reasonable field-aligned current magnitudes less than 58 μA/m^2) this gives $N^{nt}/N{>}80\%$. This is unreasonable since it is equivalent to stating that the majority of the electrons are not thermal, which is a contradiction, although it is consistent with the notion of a field-aligned potential drop of the order of only 1/2 volt V. Both results, nevertheless, contradict the starting hypothesis. If we choose instead the other solution from the electron energy balance, we would have to deal with much higher field-aligned current density, in the range 350–740 μA/m^2, but would obtain $N^{nt}/N \cong 20\%$. This may be a more realistic number for the non-thermal situation, but it still amounts only to a 2-volt drop in the region of interest. In addition, with this solution, we would have to sustain very high field-aligned current densities over a wide region of latitudes (or times).

Given that both solutions bring more problems than they solve, we are led to conclude that the third species, i.e. non-thermal electrons, scenario is not a good explanation for upwelling ions in TIU-2 events. This leaves turbulent scattering of electrons by high frequency waves as our final alternative. However, the inclusion of turbulence forces us to reprocess the thermal electron momentum and energy balances. Thus, we return to both the momentum and energy equations and consider the differences that high frequency turbulence may bring to the system.

3.4 The effect of high frequency wave-particle interactions

We propose that during the TIU-2 events, at least some of the field-aligned current is carried by ions (observed leaving the ionosphere), owing to electron deceleration by high frequency turbulent waves. This assumption suggests that we should introduce a frictional force between electrons and high frequency plasma waves in the electron momentum Eq. (1). We introduce the effect of high frequency turbulence

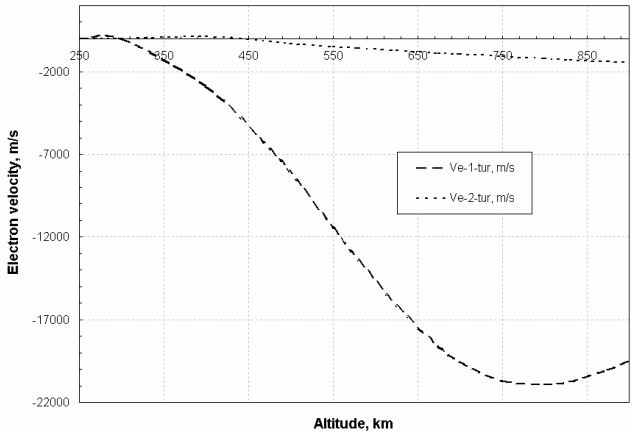

Fig. 8. Field-aligned electron velocity corresponding to the two $u_\parallel$ solutions of Fig. 5, but in the presence of high-frequency turbulence.

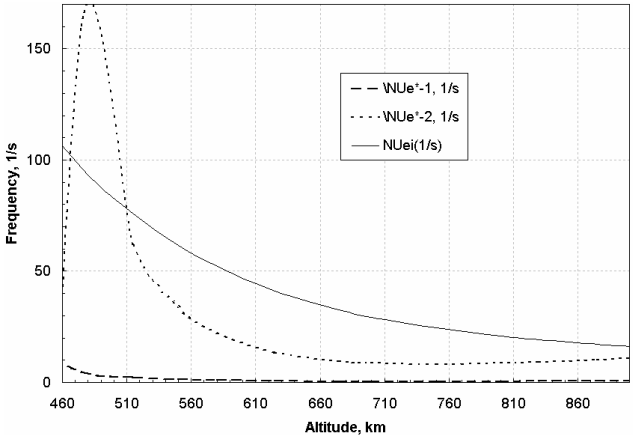

Fig. 9. Effective collision frequency for electron-wave interactions corresponding to the two $u_\parallel$ solutions from Fig. 5 in the presence of high-frequency turbulence (broken and dashed lines). The Coulomb collision frequency between electrons and ions is shown by the solid line.

through an effective collision frequency ν_e^*. Doing this presupposes that the hypothesized waves are stationary (more on this in the next section). As a result, the ion field-aligned velocity from Eq. (7) would take the form:

$$V_i \cdot b = V_{i||} = -\frac{\nabla_{||}(p_e + p_i)}{MN\nu_{in}^*} + \frac{g\cos D}{\nu_{in}^*} - \frac{m\nu_e^*}{M\nu_{in}^*} V_e \cdot b. \qquad (26)$$

The new parameter $\nu_e^* V_{e||}$ therefore has to satisfy the relation

$$\nu_e^* V_{e||} = -\frac{\nabla_{||}(p_e + p_i)}{mN} + g\cos D\frac{M}{m} - \frac{M}{m}\nu_{in}^* V_{i||}. \qquad (27)$$

The electron-turbulence interactions also have to affect the electron energy balance (Eq. 9). At the very minimum, if we assume once again that the waves interacting with the electrons are "stationary" (i.e. moving at speeds less than 1 km/s), the frictional heating contribution from the interaction of the electrons with the waves has to be given by $Nm\nu_e^* V_e^2$ (similar to the interactions that would be felt with a stationary species). Assuming that this is the only contribution from turbulence (i.e. no significant anomalous heat flow, for example) then, using the fact that $Nm\nu_e^* V_e$ is a fixed quantity related to the observations through Eq. (27) we arrive at the following modified electron energy balance:

$$A_2 u_\parallel^2 + A_1 u_\parallel + A_0 = 0, \qquad (28)$$

where the new coefficients A_j for the equation are now given by the known quantities

$$A_2 = 0.51 Nm\nu_{ei} \qquad (29)$$

$$A_1 = (1.5Nk_T\nabla_\parallel T_e - T_e k_T \nabla_\parallel N) - Nm\nu_e^* V_e \qquad (30)$$

$$A_0 = -A_1 V_{iz'} - \frac{3m}{M} N\nu_{ei} k_T (T_e - T_i) + 0.059\frac{k_T^2}{m}\left[2.5\, T_e^{3/2}\left(\frac{\partial T_e}{\partial z'}\right)^2 + T_e^{5/2}\frac{\partial^2 T_e}{\partial z'^2}\right]. \qquad (31)$$

Our two new solutions for the current velocities are very similar to what we had obtained without the turbulent contributions. This can easily be seen by comparing in Fig. 5 the dashed line with the line linked by triangles and the dotted line with the line linked by squares. The dashed and dotted lines are the results obtained with the inclusion of turbulence while the triangles, and squares are from original solution discussed earlier. Likewise, the results for the current densities themselves are not modified greatly by the presence of turbulence, as can be seen from Fig. 6 where we used the same kind of display as in Fig. 5 to intercompare various solutions.

A similar format is also used in Fig. 7, this time to compare the electric field solutions. Figure 7 clearly shows that, once again, the modifications to the calculated field-aligned electric field that are introduced by the turbulent contributions are indeed minor. The final parameters derived from our analysis are the field-aligned electron velocity, using $V_{e\parallel}$=$V_{i\parallel}$−$u_\parallel$, and the effective collision frequency, which in turn is easy to determine using Eq. (21), once we know the field-aligned electron drift. These results are displayed in Figs. 8 and 9. They show the electrons counterstreaming with the ions. The electrons are also drifting at speeds not even twice as large as those of the ions. The parallel electric field is also relatively modest, of the order of 1 μV/m. Finally, the wave-induced electron collision frequency is of the same order of magnitude as the electron-ion collision frequency.

Finally, we recall that we have assumed that the waves responsible for electron scattering were "stationary", i.e. slowly moving. If they had been drifting, we would have $-mN\nu_e^*(V_{e\parallel} - V_{w\parallel})$ replacing $-Nm\nu_e^* V_e$ in the modified electron momentum, where $V_{w\parallel}$ is the wave speed. This term would still have had to balance the RHS of Eq. (21) (times Nm), that is, would still be such as to account for the observed ion drift. However, the determination of the anomalous collision frequency would be affected by the wave speed.

Turning to the energy equation next, the extra term on the right-hand side of Eq. (24) would be unaffected, while the wave drift would modify the $V_{i\|}$ term, which would now contain $(V_{i\|}-V_w)$ instead of just $V_{i\|}$. Since the RHS of Eq. (31) is dominated by the second (electron cooling) and third (electron heat conduction) terms, this means that, for wave drifts less than a few km/s, neither the derived electric fields nor the electron drifts would be affected much. Within this limit of a few km/s, however, the wave speed has to be considered a free parameter of the problem that, in the present analysis, affects our extraction of the magnitude of the anomalous electron collision frequency more than anything else.

Therefore, we reach the surprising conclusion that, in the end, rather large, km/s, ion outflows can be achieved with just a little bit of quasi-stationary turbulence to slow down the electrons, and with a rather modest field-aligned electric field (in comparison with the regular ambipolar field) to accelerate the charged particles.

3.5 Origin of the field-aligned electric field

The final part of the riddle requires finding a common origin for the stationary waves and for the parallel electric field, modest as they both might be. To this end, we have reexamined the observations by Wahlund et al. (1992) and related events, looking for additional clues. One feature that we found is that TIU-2 events were accompanied by a southward motion of the auroral arc, similar to the events reported by Forme et al. (1995). Specifically, for the particular TIU-2 event studied in detail here, we could determine that the southward velocity of the arc was of the order of 220 m/s.

We propose that the southward motion of the arc which actually forces the east-west convection electric field that pushes the arc south, is also responsible for the generation of the field-aligned electric field. In addition, we suggest that this phenomenon is part of a stationary Alfvén wave pattern generation, which would explain why the turbulence appears to be stationary.

We use Fig. 10 to illustrate and answer the conversion question first. As the diagram illustrates, the magnetic perturbation associated with the precipitation-induced field-aligned currents in a single, isolated, east-west arc will be tilting the magnetic field towards the east on the equatorward side of the arc. The component of the electric field that drives the arc south will have, on the other hand, to point west. This means that a small part of the horizontal (originally "perpendicular" prior to the arc appearance) electric field will now have an upward component. This upward component will indeed drive the ions upward and the electrons downward, and heat the electrons (Erukhimov and Kagan, 1994; Kagan et al. (1996), just as we have seen/deduced from the observations. Again, from the simple geometry shown in Fig. 10 we can see that the parallel field should originally be equal to $E_{0x}b_x$, where b_x is the east-west magnetic perturbation B_x divided by the total magnetic field B_0. However, through the very field-aligned currents that we have inferred, the actual parallel field would have to be less than $E_{0x}b_x$ which should therefore be considered as an upper limit. This is indeed what we find.

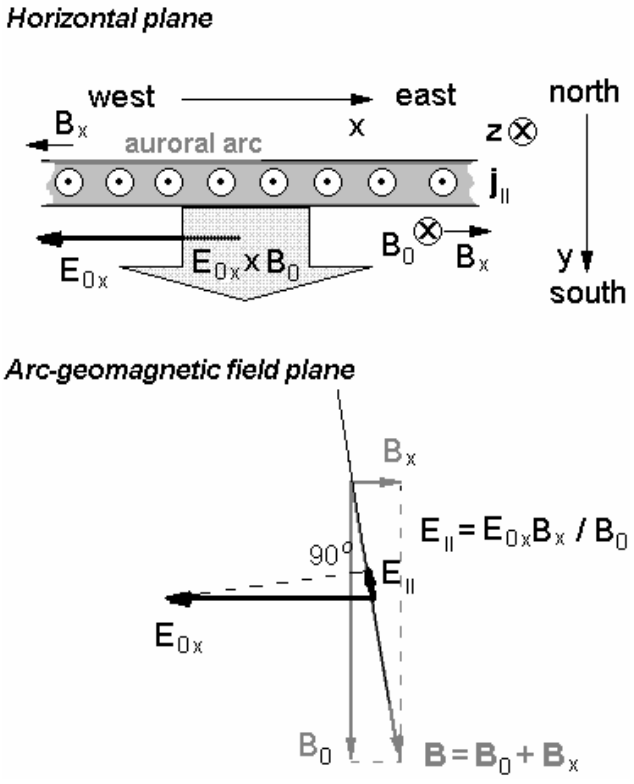

Fig. 10. Schematic diagram describing the formation and role of parallel electric fields in the presence of a single, isolated, north-south moving arc. The arc is assumed to extend in the magnetic east-west direction. A westward component of the electric field in the Northern Hemisphere produces an equatorward drift for the arc (horizontal plane). With upward currents the magnetic perturbation on the equatorward side is pointing to the east. The arc-geomagnetic field plane (which greatly exagerates the perturbed magnetic field component) shows that the westward electric field acquires an upward component parallel to the total magnetic field. In the absence of a complete shielding by the electrons (see text), this field is such as to expel ionospheric ions, i.e. to push them upward.

In terms of magnitude, we recall that magnetic perturbations of the order of 100 nT can easily be expected around arcs (e.g. Fig. 3). In addition, for our case study, the southward drift velocity of $V_D \cong 220$ m/s implies a westward convection electric field $E_x \cong -10$ mV/m. This produces an upward $E_{||}=E_x\, b_x$ of the order of 20 μV/m, using our 100 nT for the magnetic perturbation. This is one order of magnitude greater than the 1 μV/m that we obtained from our analysis and consistent with the expectation of at least a partial shorting out of $E_{||}=E_x b_x$ by the very thermal currents that we have inferred. The high frequency turbulence itself might also be generated by the large current densities found immediately following the occurrence of the parallel field. In effect, the decay of the high frequency turbulence on a field line would therefore be responsible for the remnant electric fields and the ion outflows.

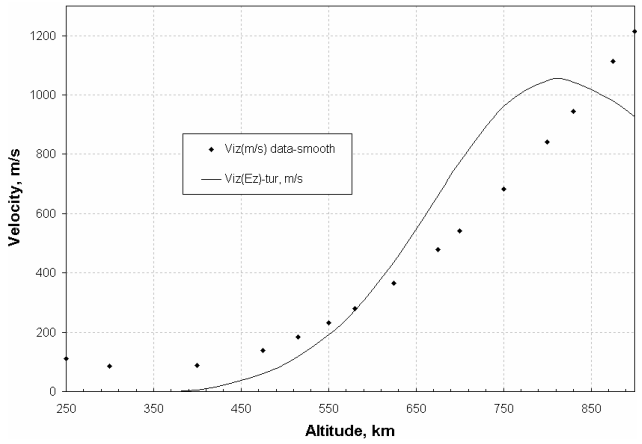

Fig. 11. Field-aligned ion velocity: measured (black dots) and obtained from the field-aligned electric field described by the dotted line in Fig. 7 (solid line).

Our TIU-2 scenario reminds us of the stationary inertial Alfvén waves scenario thought to be responsible for auroral arc formation, at least sometimes (Knudsen, 2001). This model is similar to the notion of stationary Alfvén waves (Seyler, 1990; Knudsen, 1996), except that the southward drift of the arc across the geomagnetic field replaces the role of time variations and leads to the field-aligned electric field and the stationary turbulence. According to the stationary Alfvén waves picture, a steady-state electron acceleration is produced within multiple parallel sheets along the geomagnetic field lines. The plasma drift across the stationary structures therefore replaces the role of time variations and leads to field-aligned electric fields.

4 Discussion and conclusions

From our study of the data, we have evolved the following scenario for the class of ionospheric ion outflows referred to as TIU-2 in this paper. We first obtain a conversion of a small part of the perpendicular westward component of the electric field, into a field-aligned electric field as a result of the westward magnetic perturbation associated with an arc. The partial conversion of the westward electric field into a field-aligned electric field is sustained by the very southward motion of the auroral arc that is triggered by the westward electric field. The field-aligned electric field thus generated provides counterstreaming of electrons and ions in which the ions go up and the electrons go down. The presence of turbulence slows the electrons down, which in turn enhances the ion motion. In our case study, the current densities reach values of the order of $50\,\mu\mathrm{A/m}^2$ in the process. At the same time, the electrons are heated, partly through friction, and in our case study, mostly through heat advection. This produces the large increases in electron temperatures that accompany the TIU-2 events.

For the case that we have studied in detail, the ion outflow reaches 1.2 km/s near 900 km altitude and is predominantly due to the field-aligned electric field. This is illustrated in Fig. 11, where we compare the ion outflow computed from our field-aligned electric field with the velocities that were actually observed.

As far as we can tell, the above analysis of a TIU-2 event is the first one to have investigated the electron energy balance as a key element to the solution of the problem. The energy balance was what led us to conclude that a field-aligned electric field is indeed responsible for the observed electron temperature increases accompanying this type of ion outflow. Another novel aspect of our study is our suggestion that quasi-stationary high frequency turbulence has to be ultimately responsible for the observed ion outflows by impeding the shorting action of the electrons. A final new contribution is with respect to the origin of the field-aligned electric field, which we have linked to the perpendicular electric field conversion described in Fig. 10.

It is worth noting that the type-2 ion outflows described here precede, as a rule, the more extreme case of TIU-2 events where enhanced ion-acoustic lines are observed (Anja Strømme, private communication). This connection could possibly have something to do with the high frequency turbulence that we have inferred from our analysis. In particular, Forme (1993) has proposed that strong high frequency Langmuir turbulence could be at the origin of the enhanced ion-acoustic lines through a mode-coupling mechanism. It also seems likely that the system, through the field-aligned electric field mechanism suggested here, could generate field-aligned electric fields much stronger than the $1\,\mu$V/m that we deduced for our particular case study and correspondingly larger field-aligned current densities. We have seen that fields 20 times larger could be triggered along arcs without much difficulty. This could lead to a much stronger counterstreaming of electrons with ions and much greater electron temperatures. As mentioned in the review by Sedgemore-Schelthess and St.-Maurice (2001) the stronger electric fields can also generate topside current instabilities (e.g. Kindel and Kennel, 1971) which, in turn, would ultimately destabilize the ion-acoustic lines that have been seen under conditions similar to type-2 TIU events (e.g. Rietveld et al., 1991; Wahlund et al., 1992; Forme et al., 1995; Forme and Fontaine, 1999).

Appendix A Correctness of T_e interpolation

In Fig. A1 we show that equivalently good fits for T_e, second polynomial and logarithmic (upper panel), give very different results for the gradient of heat flux involving second derivatives (lower panel). In the lower panel of Fig. A1 we show the gradient of heat flux calculated accordingly to the formula using the second derivative of T_e interpolated as a second polynomial fit (curve with hollow circles) and taking the derivative of the heat flux after interpolating it with another polynomial fit (curve with full circles). One can see that the results are very different while the same procedure

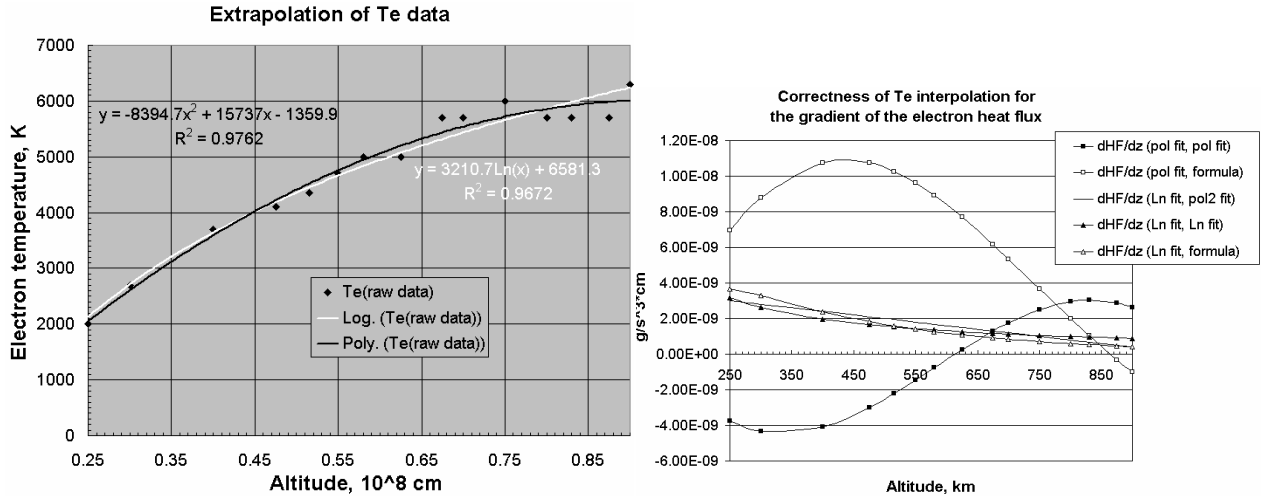

Fig. A1. Illustration of correctness of T_e interpolation.

made for the logarithmic fit shows very close results for the second derivative calculated using the formula (curve with hollow triangles) and interpolation of the heat flux via either a second polynomial (solid curve) or logarithmic (curve with full triangles) fits.

Acknowledgements. This research was supported by the Canadian Natural Sciences and Engineering Research Council, which includes funding for the e-POP project. LKM's research was also funded in part by the Russian Foundation of Basic Investigations grant 01-05-65025. The authors are grateful to R. T. Tsunoda for his initial involvement in this work. They also thank Drs Schlegel, Blelly, Moorcroft, MacDougall, Forme and Semeter for helpful discussions on the EISCAT and Sondrestrom data.

Topical Editor M. Lester thanks a referee for his help in evaluating this paper.

References

Boehm, M. H., Carlson, C. W., McFadden, J. P., Clemmons, J. H., and Mozer, F. S.: High-resolution sounding rocket observations of large-amplitude Alfvén waves, J. Geophys. Res., 95, 12 157–12 171, 1990.

Erukhimov, L. M. and Kagan, L. M.: Thermomagnetic effects in ionospheric plasma, J. Atmos. Terr. Phys., 56, 133–140, 1994.

Forme, F. R. E.: A new interpretation on the origin of enhanced ion acoustic fluctuations in the upper ionosphere, Geophys. Res. Lett., 20, 2347–2350, 1993.

Forme, F. R. E., Fontaine, D., and Wahlund, J. E.: Two different types of enhanced ion acoustic fluctuations observed in the upper ionosphere, J. Geophys. Res., 100, 14 625–14 636, 1995.

Forme, F. R. E. and Fontaine, D.: Enhanced ion acoustic fluctuations and ion outflows, Ann. Geophys., 17, 182–189, 1999, **SRef-ID: 1432-0576/ag/1999-17-182**.

Foster, C., Lester, M., and Davies, J. A.: A statistical study of diurnal, seasonal and solar cycle variation of F-region and topside auroral outflows observed by EISCAT between 1984 and 1996, Ann. Geophys., 16, 1144–1158, 1998, **SRef-ID: 1432-0576/ag/1998-16-1144**.

Hultqvist, B.: Extraction of ionospheric plasma by magnetospheric processes, J. Atmos. Terr. Phys., 53, 3, 1991.

Iijima, T. and Potemra, T. A.; The amplitude distribution of field-aligned currents at northern high latitudes observed by Triad, J. Geophys. Res., 81, 5971–5979, 1976.

Kagan, L. M., Kelley, M. C., and Doe, R. A.: Ionospheric electric heating by structured electric fields: Theory and experiment, J. Geophys. Res., 101, 10 893–10 907, 1996.

Kindel, J. M. and Kennel, C. F.: Topside current instabilities, J. Geophys. Res., 76, 3055, 1971.

Knudsen, D. T.: Spacial modulation of electron energy and density by nonlinear stationary Alfvén waves, J. Geophys. Res., 101(A5), 10 761–10 772, 1996.

Knudsen, D. T.: Structure, Acceleration, and Energy in Auroral Arcs and the Role of Alfvén Waves, Space Science Reviews, 95(1–2), 501–511, 2001.

Liu, H., Ma, S.-Y., and Shlegel, K.: Diurnal, seasonal and geomagnetic variation of large field-aligned ion upflows in the high-latitude ionospheric F-region, J. Geophys. Res., 106, 24 651–24 661, 2001.

Loranc, M., Hanson, W. B., Heelis, R. A., and St.-Maurice, J.-P.: A morphological study of vertical ionospheric flows in the high-latitude F-region, J. Geophys. Res., 96, 3627–3646, 1991.

Loranc, M. and St.-Maurice, J.-P.: A time dependent gyro-kinetic model of thermal ion upflows in the high-latitude F-region, J. Geophys. Res., 99, 17 429–17 451, 1994.

Rietveld, M. T., Collis, P. N., and St.-Maurice, J.-P.: Naturally enhanced ion acoustic waves in the auroral ionosphere observed with the EISCAT 933-MHz radar, J. Geophys. Res., 96, 19 291–19 305, 1991.

Sedgemore-Schelthess, F. and St.-Maurice, J.-P.: Naturally enhanced ion-acoustic spectra and their interpretation, Surveys in Geophysics, 22, 55–92, 2001.

Seyler, C. E.: A mathematical model of the structure and evolution of small-scale discrete auroral arcs, J. Geophys. Res., 95, 17 199–17 215, 1990.

Shelley, E. G., Johnson, R. G., and Sharp, R. D.: Satellite observations of energetic heavy ions during a geomagnetic storm, J. Geophys. Res., 77, 6104, 1972.

Shunk, R. W. and Nagy, A. F.: Ionospheres: Physics, Plasma Physics and Chemistry, Cambridge University Press, 2000.

Tsunoda, R. T., Livingston, R. C., Vickrey, J. F., Heelis, R. A., Hanson, W. B., Rich, F. J., and Bythrow, P. F.: Dayside observations of thermal-ion upwellings at 800-km altitude: An ionospheric signature of the cleft ion fountain, J. Geophys. Res., 94, 15 277–15 290, 1989.

Wahlund, J. E. and Opgenoorth, H. J.: EISCAT observations of strong ion outflows from the F-region ionosphere during auroral activity: preliminary results, Geophys. Res. Lett., 16, 727–730, 1989.

Wahlund, J. E., Opgenoorth, H. J., Häggström, I., Winser, K. J., and Jones, G. O. L.: EISCAT observations of topside ionospheric ion outflows during auroral activity: revisited, J. Geophys. Res., 97, 3019–3037, 1992.

Whalen, B. A., Bernstein, W., and Daly, P. W.: Low altitude acceleration of ionospheric ions, Geophys. Res. Lett., 5, 55, 1978.

Wilson, G. R.: Kinetic modeling of O^+ upflows resulting from $\boldsymbol{E}\times\boldsymbol{B}$ convection heating in the high-latitude F-region ionosphere, J. Geophys. Res., 99, 17 453–17 466, 1994.